Energy and Power Engineering, **2010, 2, 262-270**
doi:10.4236/epe.2010.24038 Published Online November 2010 (http://www.SciRP.org/journal/epe)

Novel Control Strategy for Multi-Level Active Power Filter without Phase-Locked-Loop

Guojun Tan, Xuanqin Wu, Hao Li, Meng Liu
School of Information and Electrical Engineering, China University of Mining and Technology, Xuzhou, China
E-mail: *gjtan@cumt.edu.cn,cumt_wuxuanqin@163.com*
Received June 13, 2010; *revised August* 9, 2010; *accepted September* 21, 2010

Abstract

Active power filter (APF) using novel virtual line-flux-linkage oriented control strategy can not only realizes no phase-locked-loop (PLL) control, but also achieves a good inhibitory effect to interfere. However, there are some problems in the conventional method, such as the error of amplitude, the shift of phase angle and the non-determinacy of initial oriented angle. In this paper, two one-order low-pass filters are adopted instead of the pure integrator in the virtual line-flux-linkage observer, which can steady the phase and amplitude. Furthermore, an original scheme of harmonics detection under the rotating coordinate is advanced based on the simplified space vector pulse width modulation (SVPWM) strategy. Meanwhile, by using the new SVPWM algorithm, the voltage space vector diagram of the three-level inverter can be simplified and applied into that of two-level inverter, and this makes the control for Neutral Point potential easier.

Keywords: Active Power Filter, Harmonics Detection, Virtual Line-Flux-Linkage Observer, Active Power Filter Control without Phase-Locked-Loop, Space Vector Pulse Width Modulation

1. Introduction

The use of nonlinear loads such as power electronic devices leads to serious harmonics pollution and lager voltage fluctuation. Moreover, lager unbalance voltage and current distortions in the power system are harmful to the electrical equipment and power systems. Shunt active power filter (SAPF) can well compensate the harmonic whose frequency and amplitude both changes, and it is also recognized as an effective way to manage the grid harmonic, to reactive power pollution and to improve the quality of the power. Active power filter (APF) is a new power electronics device for dynamic harmonics restriction and reactive compensation without influenced by system inductance [1,2], besides it has such functions: adaptive ability for the parametric variation of system and load, automatic tracing and compensation for the varying harmonics [3,4]. There are some remarkable advantages in nature of three-level APF, such as lower distortion of output waveform, lower endure voltage and less switch loss, high efficiency and low electromagnetic interference (EMI), so it helps to raise the installed capacity and improves the harmonics compensation effect as well as system reliability.

On the one hand, the traditional harmonic current detection which is based on instantaneous reactive power adopts phase-lock-loop (PLL) to acquire the voltage vector angle [5-7], when the grid voltage fluctuation is more serious, PLL will be in unlocked condition because of the larger frequency offsets which can not accurately track the phase position. To solve the problem, this paper uses the virtual line-flux-linkage orientation to observe the vector angle, which converts the observation of vector angle to the flux. By using the voltage integral on the AC side of the active filter to estimate the grid flux, PLL can be omitted; meanwhile, the power grid interference can be inhibited well. On the other hand, the traditional harmonic current detection requires that the integrated vector combined by the sine and cosine function should be synchronous and phase coincidence to the integrated vector of the three-phase positive sequence fundamental voltage, otherwise, the detection accuracy of the fundamental positive sequence reactive component will be affected by phase difference [8]. Therefore, the harmonic detection principle based on the rotating coordinates is proposed in this paper. The application of virtual flux in active filter system also includes controlling generation of compensation current, so it has a very good control to harmonic current detection and compensation current ge-

neration, and the voltage space vector modulation strategy SVPWM (Space Vector Pulse Width Modulation) can be easily applied to active filter control.

In this paper, the simplified three-level SVPWM with neutral point potential adaptive control is applied to control multi-level active filter, based on this, a novel multi-level voltage active filter phase reconstruction algorithm is proposed.

2. Mathematical Model for Three-Level APF and the Rotating Coordinate Based Harmonics Detection Diagram

Figure 1 is the main circuit of NPC three-level APF, while vector diagram of the virtual line-flux-linkage oriented system is shown in **Figure 2**. When the virtual line-flux-linkage is at d axis, then mathematical model of three-level APF is in dq reference frame [9,10]:

$$Z\dot{X} = AX + Be \tag{1}$$

where:

$$Z = diag\begin{bmatrix} L_s & L_s & C_d & C_d & 0 \end{bmatrix} \tag{2}$$

$$A = \begin{bmatrix} 0 & \omega L_S & -S_{1d} & S_{2d} & 0 \\ -\omega L_S & 0 & -S_{1q} & S_{2q} & 0 \\ S_{1d} & S_{1q} & 0 & 0 & -1 \\ -S_{2d} & -S_{2q} & 0 & 0 & -1 \\ 0 & 0 & 1 & 1 & 0 \end{bmatrix} \tag{3}$$

$$X = \begin{bmatrix} i_d & i_q & V_{dc1} & V_{dc2} & 0 \end{bmatrix}^T \tag{4}$$

$$B = diag\begin{bmatrix} 1 & 1 & 0 & 0 & 0 \end{bmatrix} \tag{5}$$

$$\begin{bmatrix} e_d \\ e_q \end{bmatrix} = \begin{bmatrix} 0 \\ E_m \end{bmatrix} \tag{6}$$

In (2) to (6),

L_s: AC side inductance of APF; C_d: capacitance of DC side; E_m: peak voltage of power system; i_d, i_q: the D-axis and Q-axis AC current of APF; V_{dc1}, V_{dc2}: the upper and down DC voltage relevant to neutral point; $S_{1d}, S_{1q}, S_{2d}, S_{2q}$: the D-axis and Q-axis components of switching function.

According the virtual line-flux-linkage oriented strategy showed in **Figure 2**, the reference compensation current can be obtained:

$$\begin{cases} i_{dh}^* = \tilde{i}_{Ld} \\ i_{qh}^* = \tilde{i}_{Lq} \end{cases} \tag{7}$$

$$\begin{cases} \tilde{i}_{Ld} = i_{Ld} - \bar{i}_{Ld} \\ \tilde{i}_{Lq} = i_{Lq} - \bar{i}_{Lq} \end{cases} \tag{8}$$

where:

i_{Ld}, i_{Lq}: The D-axis and Q-axis current of nonlinear load;

$\bar{i}_{Ld}, \bar{i}_{Lq}$: The D-axis and Q-axis fundamental current of nonlinear load through low pass filter from i_{Ld}, i_{Lq};

$\tilde{i}_{Ld}, \tilde{i}_{Lq}$: The D-axis and Q-axis component harmonics current of nonlinear load.

3. The diagram of Novel Virtual Line-Flux-Linkage Observer

The essence of virtual line-flux-linkage oriented method is to gain accurate space angle (θ) estimation of the oriented vector $\vec{\psi}$, as shown in **Figure 2**, the angle can be obtained:

$$\begin{cases} \sin\theta = \psi_\beta \Big/ \sqrt{\psi_\alpha^2 + \psi_\beta^2} \\ \cos\theta = \psi_\alpha \Big/ \sqrt{\psi_\alpha^2 + \psi_\beta^2} \end{cases} \tag{9}$$

Then the estimation of θ is converted to the evaluation of α and β components of the virtual line-flux-linkage.

$$\begin{cases} e_\alpha = L\dfrac{di_\alpha}{dt} + v_\alpha \\ e_\beta = L\dfrac{di_\beta}{dt} + v_\beta \end{cases} \tag{10}$$

In (10), v_α and v_β are the α, β voltage quantity at AC side of three-phase APF, respectively. Integrated both sides of (10),

$$\begin{cases} \psi_\alpha = \int v_\alpha dt + Li_\alpha \\ \psi_\beta = \int v_\beta dt + Li_\beta \end{cases} \tag{11}$$

ψ_α, ψ_β: α, β value of virtual line-flux-linkage.

It can be seen from (11) that the flux linkage can be evaluated by the voltage integral at AC side of APF, while it brings a problem of the integral initial value which cause an error of the flux linkage, furthermore, the method of pure integrator doesn't retrain the DC component of the input signal, even a little DC component can make the integrator saturation. In this manner, the flux linkage in $\alpha\beta$ axes can be a circular trajectory with DC offset corresponding to the centre of the circle, meanwhile, it cause the inaccuracy of virtual line-flux-linkage oriented angle and impact both the authenticity of current feedback and the veracity of voltage space

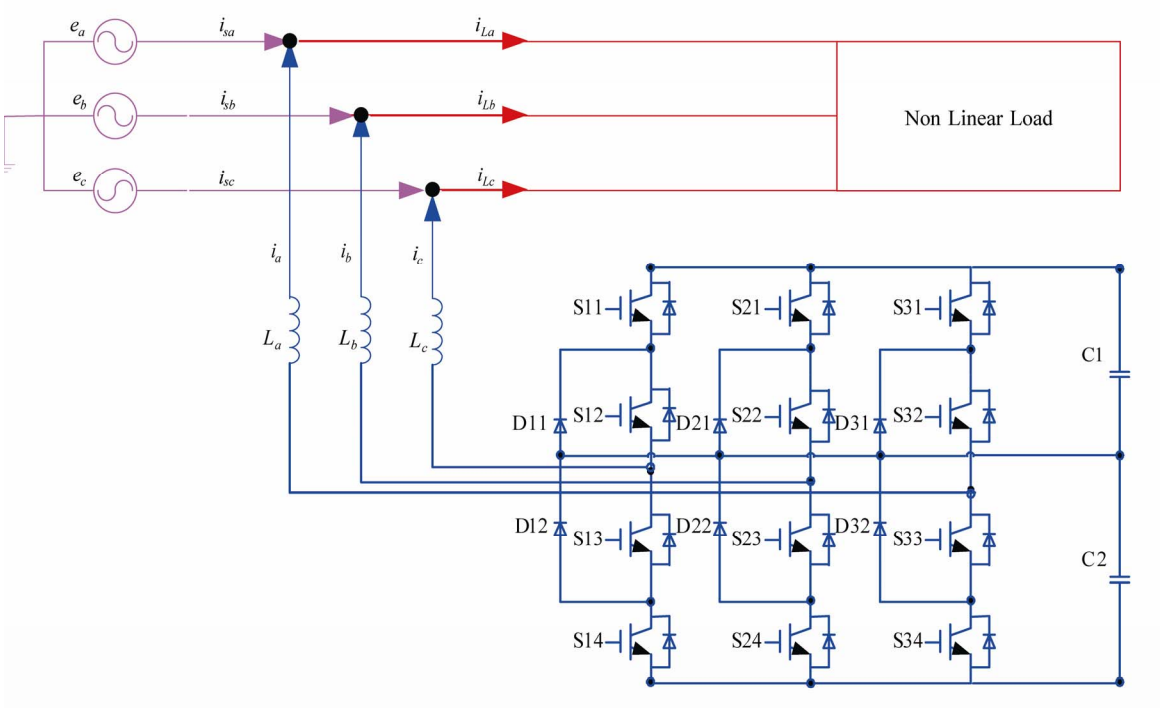

Figure 1. Topology of a diode NPC three-level shunt APF.

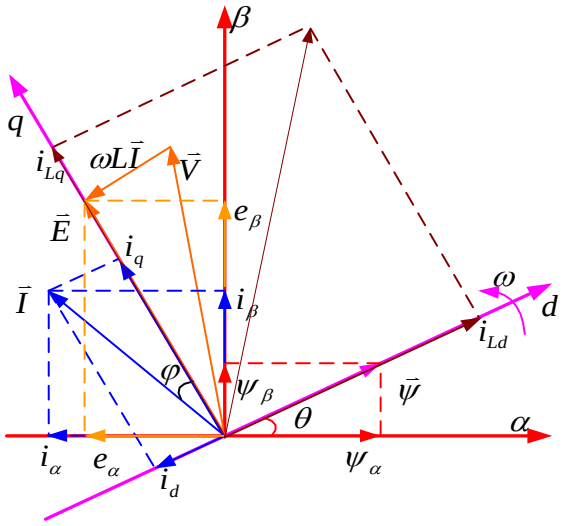

Figure 2. Vector diagram of the virtual line-flux-linkage oriented system.

vector supply, and even aggravate the performance of APF seriously. As a result, it brings large current shock in the process of starting, and even can't start. Therefore, in order to achieve an accurate flux estimate, it's necessary to make some measures to eliminate influence of the integral initial value.

In the traditional virtual flux estimation, in order to solve initial value problems of pure integrator, it usually use the first order inertia filter ($\frac{1}{s+\omega_f}$) instead of the pure integrator ($\frac{1}{s}$) in flux estimation. It can be seen from the formula of the first order filter that the first order inertia is similar to the pure integrator when the frequency ω of the sinusoidal input is far greater than ω_f.

However, it is also required that the first order inertia should have a certain decay to the direct flow, that means ω_f should be a certain value, and not too small, otherwise the decay will be very slow .So the first order low pass filter has contradictions between approximating pure points and decaying of the DC component, that means ω_f must maintain a certain value to decay, while it also should be far less than ω to approximate the integral. Know from the above analysis.

Low-pass filter is adopted by conventional virtual line-flux-linkage estimate to substitute for the purely integrator to least the DC drift, however, it would lead to errors of amplitude and phase angle. As described by the equation ($W_s = \frac{N}{s+\omega_c} \cdot \frac{N}{s+\omega_c}$), the novel virtual line-flux-linkage observer and the comparison of three observers are showed in **Figure 3** and **Figure 4** respectively. According to **Figure 4**, it is quite easy to found that the proposed algorithm respond faster than that of conventional way. It can be seen from the bode figure

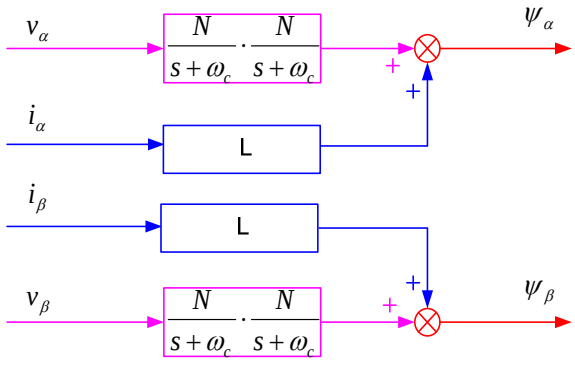

Figure 3. The novel virtual line-flux-linkage observer.

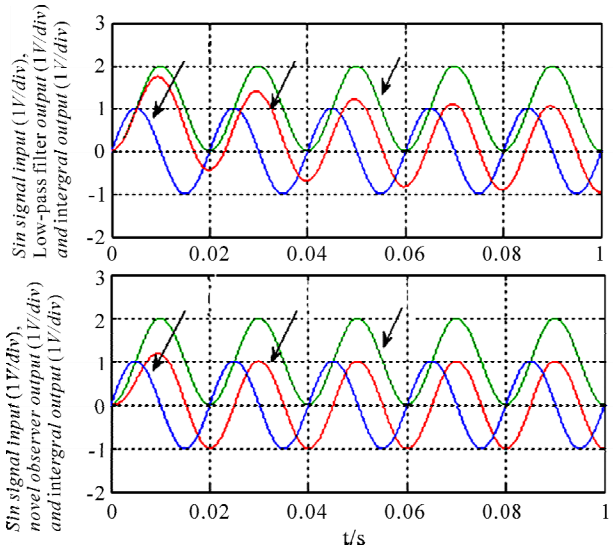

Figure 4. The comparison of the three observers.

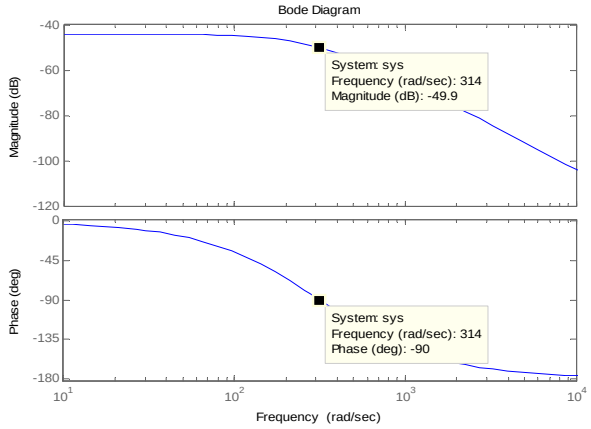

Figure 5. Bode diagram of the novel virtual line-flux-linkage observer.

that it can replace the pure integrator by making the amplitude decay 49.9db and phase shift 90° at the same time while $\omega = 314 Rad/s$.

4. The Simplified SVPWM Algorithm and Novel Voltage Estimation for Three-Level APF

In this paper, the simplified three-level SVPWM algorithm is adapted, as shown in **Figure 6**. The voltage space vector diagram of the three-level inverter can be regarded as a hexagon composed by six small two-level space vectors, and all the hexes are centered by vertexes of inner one. Hence, two-level SVPWM algorithm can be applied to calculate the duration-time and the switch sequence of voltage vector [11].

Because of inherent problem in the topology of the diode-clamping three-level converter, the various switch states have different impacts on the neutral-point potential. The middle vectors can cause neutral-point voltage deviation because of asymmetric parameter in practice. Small vectors will cause the fluctuation of neutral-point potential. There is a striking contrast effect between the two different middle vectors corresponding to different switch status vector [11].

There exist the regions that are overlapped by adjacent small hexagons as shown in **Figure 6**. So if the reference voltage vector stays at those regions, S can have any values that are possible. V_{s1_ref} is the corrected reference voltage vector when the index S has the value of 1, and V_{s2_ref} is the corrected reference voltage vector when the index S has the value of 2. If the two-level plane of S = 1 is selected, the switching sequence decided by reference voltage vector is given as follows:

$$V_{1N}(0\,-1\,-1) \rightarrow V_{2N}(0\,0\,-1) \rightarrow V_8(1\,0\,-1) \rightarrow V_{1P}(0\,-1\,-1)$$

V_{1N}, V_{2N} are respectively voltage space vectors of the corresponding switching sequence (0-1-1) and (0 0-1), and they are both negative short vectors; V_{1P} (1 0 0) is a positive short vector voltage space vector. T_{1N}, T_{2N}, T_8, T_{1P} are dwelling times of the corresponding voltage vectors. The voltage vector V_{1N} and V_{1P} have the same output voltage V_1, and dwelling times of the V_{1N}, V_{1P} are equal. If the above switching sequence is adopted, the dwelling time of negative short vectors is longer than the positive ones; neutral-point potential will decline. If the two-level plane of S = 2 is selected, the switching sequence is given as follows:

$(0\,0\,-1) \rightarrow (1\,0\,-1) \rightarrow (1\,0\,0) \rightarrow (1\,1\,0)$, the dwelling time of negative short vectors is shorter than the positive ones, neutral-point potential will rise. So the neutral-point potential can be controlled by changing the corresponding the value of index S.

As can be seen from (11), on the basis of the proposed algorithm, the voltage at the terminals of three-level rectifier is estimated, which is shown in **Figure 7**.

When the reference voltage is in the first sector, esti-

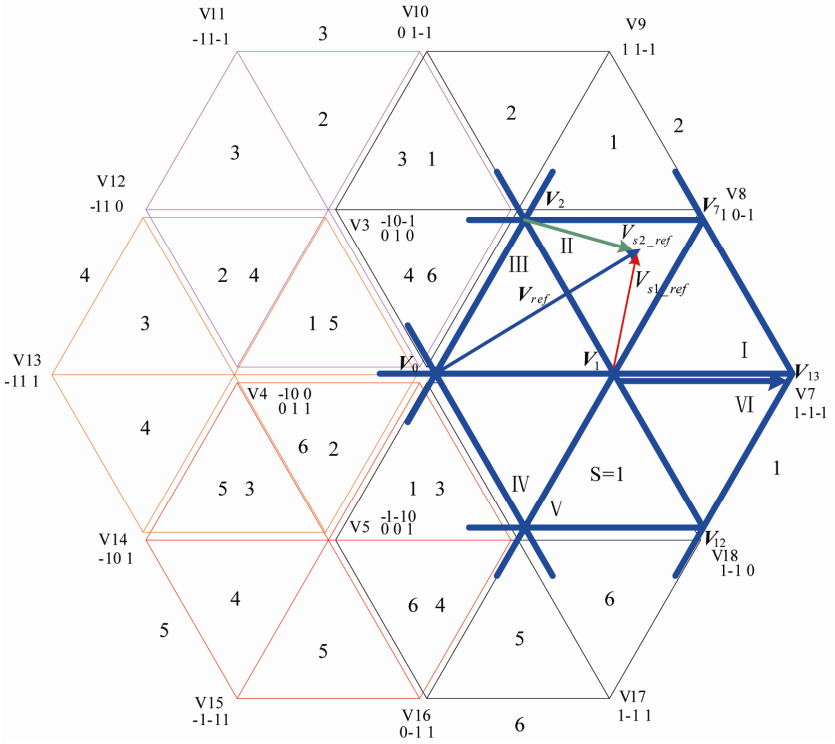

Figure 6. The simplified three-level SVPWM algorithm.

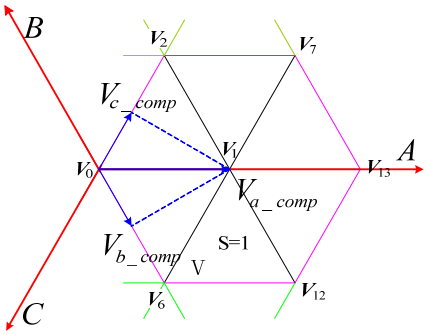

Figure 7. The novel three-level voltage estimation algorithm.

mated three-phase voltages are given by:

$$\begin{cases} u_{acalc} = \frac{1}{3}\times u_{dc} + \frac{1}{3}\times u_{dc}(\frac{2}{3}t_{aon} - \frac{1}{3}t_{bon} - \frac{1}{3}t_{con}) \\ u_{bcalc} = -\frac{1}{3}\times u_{dc}\times\cos(60°) + \frac{1}{3}\times u_{dc}(\frac{2}{3}t_{bon} - \frac{1}{3}t_{aon} - \frac{1}{3}t_{con}) \\ u_{ccalc} = -\frac{1}{3}\times u_{dc}\times\cos(60°) + \frac{1}{3}\times u_{dc}(\frac{2}{3}t_{con} - \frac{1}{3}t_{aon} - \frac{1}{3}t_{bon}) \end{cases} \quad (15)$$

where, u_{acalc}, u_{bcalc}, u_{ccalc} are the estimated voltage of three-level rectifier. u_{dc} is DC bus voltage of three-level rectifier. t_{aon}, t_{bon}, t_{con} are the duration-time of three-phase for two-level algorithm, respectively.

5. The Main Circuit Design and Experimental Results Analysis

To verify the viability of proposed non PLL control scheme for multi-level APF and evaluate performance of this method, the test platform is established and operated, and its control sketch is showed in **Figure 9**. As shown in **Figure 10**, the structure of full-digital controller is composed of DSP (TMS320F2812 of TI) and FPGA. The system can implement DC bus voltage control, har-

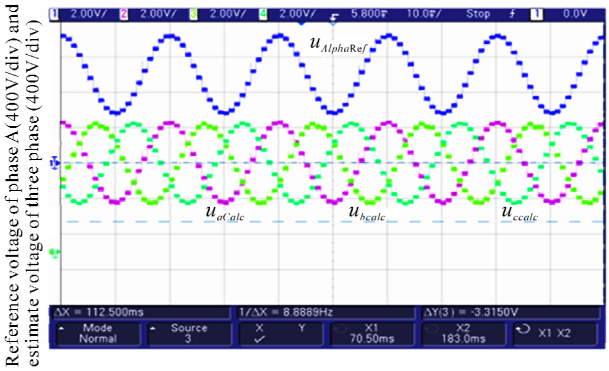

Figure 8. Experiments waveform of the novel three-level voltage estimation algorithm.

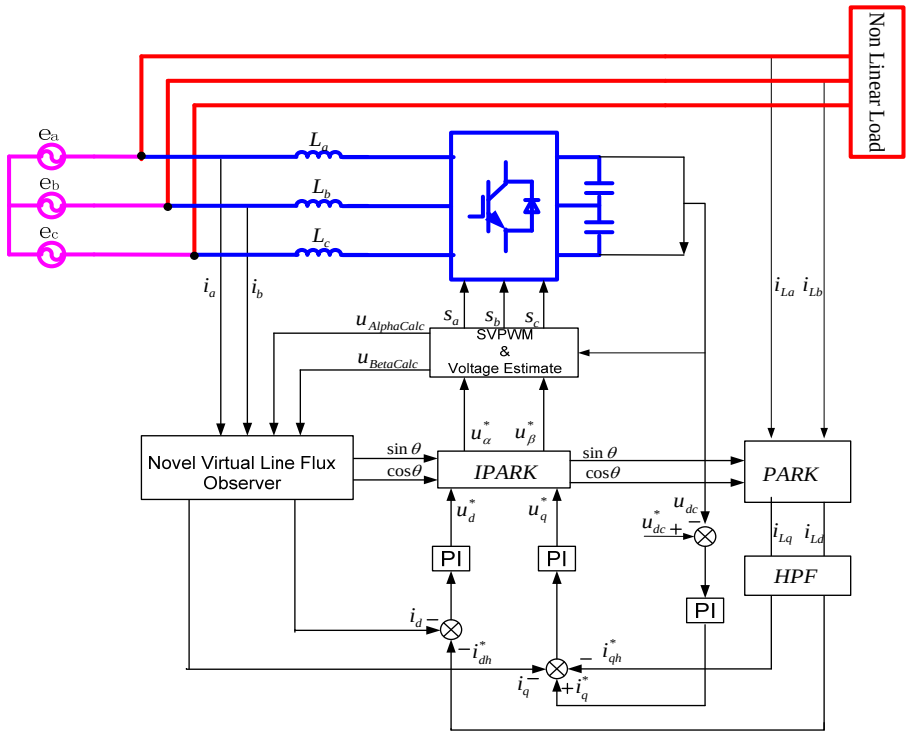

Figure 9. Novel diagram of the virtual-flux oriented vector control diagram of APF.

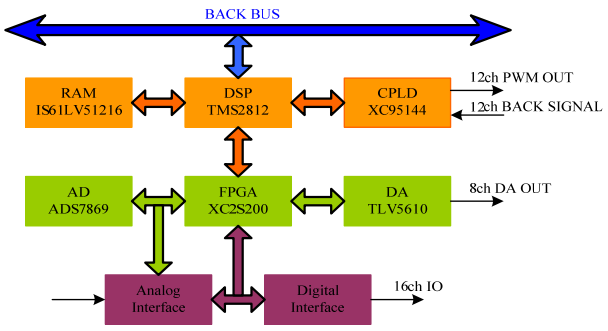

Figure 10. Structure of full-digital controller.

monics detection, closed-loop current control, fault diagnosis and etc.

5.1. The Principles of the Main Circuit Parameter Calculation

1) The design of inlet inductance on AC side

The design of AC filter inductor has two principles: for one thing, it is the power of active power filter to track and control compensation current, and make sure it can still produce a corresponding compensation current while the load current has larger current rate of change; for another, it is to satisfy the requirements of tracking the size of compensation current ripple.

It can be known from [12] that:

$$L_{\max} \le \frac{4U_{dc}}{9\times(10\sim 20)f\times 2.3I_a^*} \tag{16}$$

The maximum inductance value can be acquired by the above equation, while the minimum inductor value is determined by the size of allowable ripple current, the size of the ripple current should be limited within the prescribed range while choosing the inductor value.

$$L_{\min} \ge \frac{2U_{dc}T_s}{9\Delta i_{\max}} \tag{17}$$

Combined with (16) (17), It can be obtained:

$$\frac{2U_{dc}T_s}{9\Delta i_{\max}} \le L \le \frac{4U_{dc}}{9\times(10\sim 20)f\times 2.3I_a^*} \tag{18}$$

where, U_{dc} is the DC bus voltage; T_s is switching frequency; $\Delta i_{\max}$ is the maximum allowable value that compensation current deviate from the reference current; f is the current frequency of the fundamental wave; I_a^* is the effective reference current.

2) The design of the DC bus capacitor

Owing to both the energy pulse and switching losses caused by harmonic and reactive current in the APF compensation current and the energy pulse caused by the filter inductor energy storage on AC side, the capacitance is difficult to maintain a constant. The larger the capacitor is, the smaller such fluctuations would be, but the

capacitance value is not unlimited, so the design principles of DC bus capacitor is to work as a minimum capacitance while APF can be under normal operative condition.

It can be known from [12] that:

$$C_{\min} = \frac{S_c T}{\lambda(1+\lambda)U_{dc}^2} \tag{19}$$

$$\lambda = \frac{\Delta U_{dc\max}}{U_{dc}} \tag{20}$$

where, S_c is the compensating capacity of APF, T is the control cycle of DC bus voltage, U_{dc} is the DC voltage, λ is the voltage wave pace, $\Delta U_{dc\max}$ is the maximum allowable value of the voltage wave.

3) The controllable range of DC bus voltage

DC bus voltage selection should be considered as follows: it is not only necessary to achieve a certain current function, but also should not lead to too fierce current changes. The DC voltage threshold of three-phase APF should be greater than the peak value of AC power grid line voltage, that is $U_{dc} > \sqrt{3}E_m$, otherwise, the current can not be tracked. Take grid fluctuations and linear control range and other factors into consideration, the DC voltage can be $U_{dc} > 3E_m/\sqrt{2}$. Where, E_m is the peak value of the phase voltage on AC side.

According to the above design principles, the main circuit parameters of the APF test platform are as follow:

a) Power line voltage: 380 V/50 Hz, transformer: 380 V/120 V, and system impedance is neglected;

b) Three-phase uncontrolled rectifier bridge is adopted as the nonlinear load, its R = 8 Ω inductance L = 1.5 mH;

c) Incoming inductance of APF: L = 1.7 mH, DC bus voltage: U_d = 320 V, capacitance: C = 2300 uF.

5.2. The Experimental Results Analysis

The grid-side transformer is used to buck-boost in the high-power applications system, the effect caused by the leakage reactance of transformer can not be ignored if the non-linear load is of a large capacity or in high proportion harmonic. As can be seen in **Figure 11**, the voltage distortion caused by transformer leakage reactance makes the phase-lock-loop in unlocked condition thus it can not accurately track the phase position which caused the whole system shock. Thus, in the event that the orientation angle is not exactly, APF can not compensate the harmonic of the nonlinear loads, on the contrary, it will cause system shock.

The virtual flux observer proposed in this paper uses two first-order low-pass filters instead of pure integrator. As the integral part has characteristics of a low-pass filter, the amplitude of n times harmonic attenuate by n times of fundamental when it comes through pure integrator, which has some effect on filtering high harmonic, that is to say, the virtual flux oriented has a good inhibition on the grid voltage distortion. It can be seen from **Figure 12**, while using active filter control based on novel virtual flux, the virtual line-flux-linkage switch smoothly before and after net-side power compensation, the virtual flux angle can be able to accurately track the phase position without the effect of grid voltage distortion.

The traditional virtual line-flux-linkage uses low-pass filter instead of pure integrator which causes a certain error of amplitude and phase angle, the new virtual line-flux-linkage observer with two first-order low-pass filter instead of pure integral can be made no amplitude error and no phase shift. As can be seen in **Figure 13**, the orientation angle and amplitude errors of the virtual flux vector lead to higher current vector burr, and the novel algorithm responses faster than traditional methods which makes the current vector stabilize rapidly.

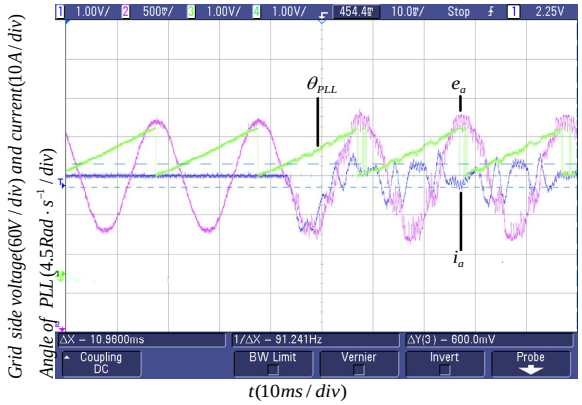

Figure 11. Control of the active filter based on phase-lock-phase.

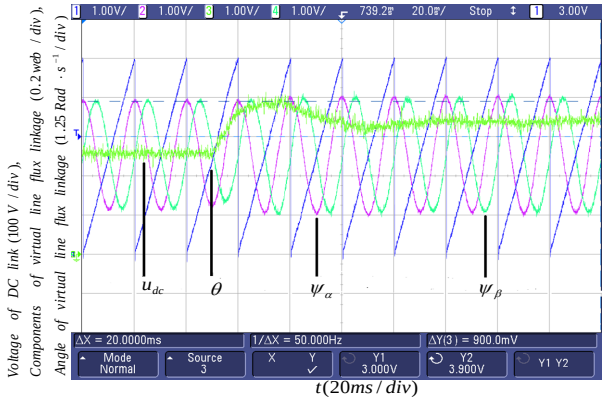

Figure 12. control of the active filter based on novel virtual flux.

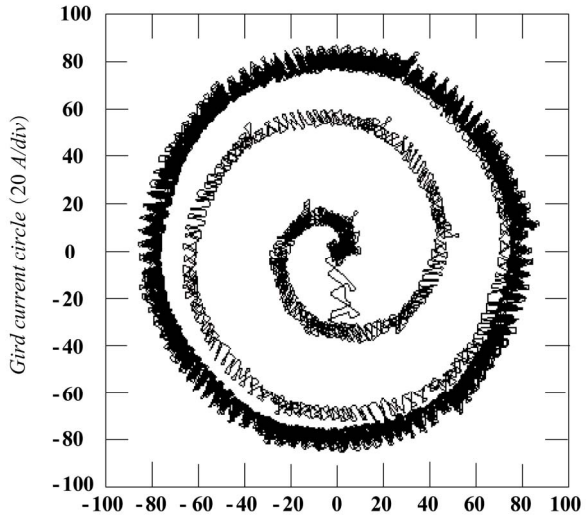

(a)

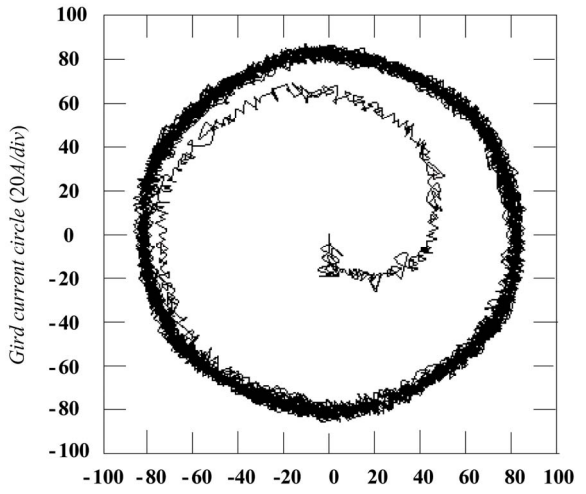

(b)

Figure 13. The vectorgraph of power current in $\alpha\beta$ axes, (a) Using low-pass filter instead of pure integrator; (b) Novel virtual flux observer.

Figure 14 shows the harmonic and fundamental wave detected by the load current rotational coordinates detection method virtual line-flux-linkage orientation based. The method realizes harmonic current detection without PLL, and compare with the traditional $i_p - i_q$ detection method PLL based, it is not restrained by frequency shift and it can omit the PLL circuit avoiding the effect that out of control of PLL brings to system of the active filter. Moreover, not only the fundamental component of the detecting current becomes more flexible but also the detection accuracy of harmonic current is higher.

Figure 15 is the final compensated line current. It is easy to found that the current is nearly close to sinusoidal and the third, fifth, seventh, ninth, eleventh and thirteenth harmonics are filtered off mostly. But there exist high harmonics by selecting the switching frequency of 2 kHz, and it is easy to be solved by the method of a high-pass filter (HPF) in parallel with the power system.

Figure 16 is the system response in the condition of abrupt change of 50% load more. The system has an excellent dynamic performance that it can be stable after 2-3 periods. According to **Figure 16(a)**, the APF based on virtual flux oriented vector control system uses a voltage outer loop and the DC bus voltage coincide with the given voltage when the system comes to be stable. The voltage amplitude fluctuation is minimal which means that there's energy exchange just between the DC side of active filter and load while the system arrive at a steady state condition. As can be seen in **Figure 16(b)**, the DC side voltage and neutral point potential fluctuation is minimal, and it shows that the strategy used in this system which is based on DC side voltage and capacitance detection and neutral point potential adaptive

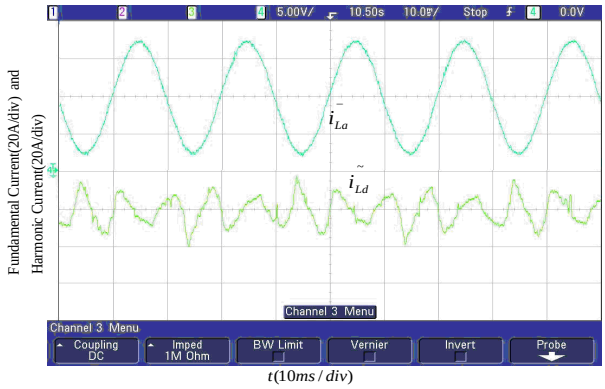

Figure 14. The harmonics current and the fundamental wave.

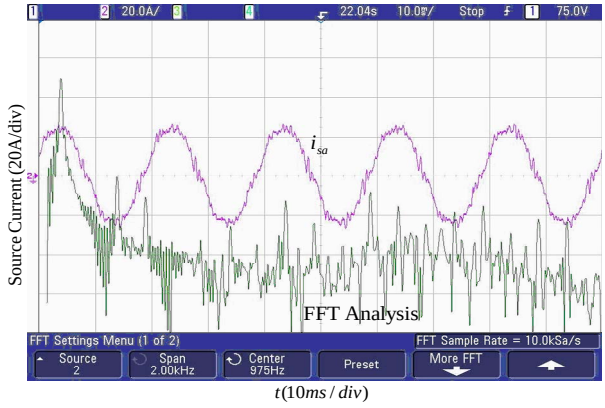

Figure 15. The compensated source current and FFT analysis.

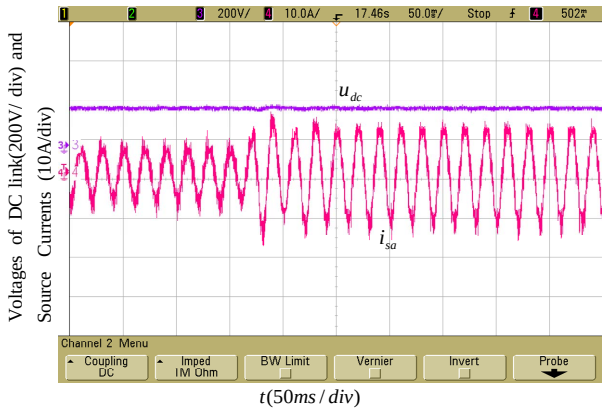

(a)

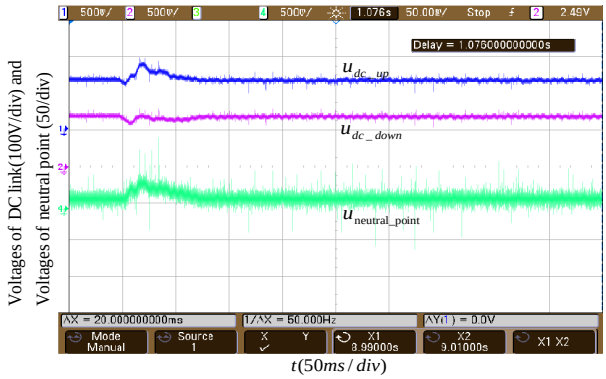

(b)

Figure 16. The dynamic response of the system, (a) The power system current and DC bus voltage response under abrupt condition; (b) DC bus voltage and neutral point potential response under abrupt condition.

compensation can effectively control the neutral-point potential both in static and dynamic operating conditions.

These results proved that the novel control algorithm with virtual line-flux-linkage-oriented based control system possess strong robustness, and also demonstrated that the simplified three-level SVPWM strategy with neutral point potential self-adaptation is valid.

6. Conclusions

The experimental results show that the scheme of adopting the proposed virtual line-flux-linkage-oriented observer can realize the non-PLL control for APF, and displayed that the load current detection under rotating coordinate oriented by virtual line-flux-linkage can not only detects harmonics current rapidly but also makes the compensating current tracked reference fast, and indicated that APF system with the method of discussed flux oriented and rotating coordinate based harmonics detection has the characteristics of decreasing line total harmonic distortion (THD) significantly and superior dynamic property, thus it is obvious that leading the simplified three-level SVPWM strategy with neutral point potential self-adaptation in control can improve the system's overall performance.

7. References

[1] M. EI-Habouk, M. K Darwish and P. Mehta, "Active Power Fliter. A Review," *IEE Proceedings of Electron Power Application*, Vol. 147, No. 7, January 2000, pp. 403-414.

[2] M. Izhar and C. M. Hadzer, "Performance for Passive Filter Inreducing Harmonics in the Distribution System," *Power and Energy Conference*, Selangor, November 2004, pp. 104-108.

[3] M. Jasinski, D. Swierczynski and M. P. Kazmierkowski, "Novel Sensorless Direct Power and Torque Control of Space Vector Modulated ac/dc/ac Converter," *IEEE International Symposium*, Vol. 2, May 2004, pp. 1147-1152 .

[4] Y. Ye, M. Kazerani, V. H. Quintana, "A Novel Modeling and Control Method for Three-Phase PWM Converters," *IEEE* 32*th Annual*, *PESC*, Vancouver, Vol. 1, June 2001, pp. 102-107.

[5] C. K. Lee, S. Y. Ron Hui and H. S.-H. Chung. "A 31-Level Casecade Inverter for Power Applications," *IEEE Transactions on Industrial Electrics*, Vol. 49, No. 3, June 2002, pp. 613-617.

[6] L. S. Czarnecki, "On Some Misinterpretation of the Instantaneous Reactive Power p-q Theory," *IEEE Transactions on PE*, Vol. 19, No. 3, May 2004, pp. 828-836.

[7] M. Malinowski, M. P. Kazmerkowski, S. Hansen, FBlaabjerg and C. D. Marques,"Virtual-Flux-Based Direct Power Control of Three-phase PWM Rectifiers," *IEEE Transactions on Industry Applications*, Vol. 37, No. 4, August 2001, pp. 1019-1027.

[8] H. Sasaki and T. Machida "A New Method to Elimate AC Harmonic Currents by Magnetic Flux Compensation Considerations on Basic Design," *IEEE Transactions on Power Application System*, Vol. 90, No. 5, 1971, pp. 2009-2019

[9] R. D. Zhao and Y. K. He, "Simulation Study on the Virtual Line Flux Oriented Vector Control of the PWM Rectifier," *Proceedings of the CSU* 2*EPSA*, Vol. 17, No. 5, October 2005, pp. 94-98.

[10] H. Sasaki and T. Machida "A New Method to Elimate AC Harmonic Currents by Magnetic Flux Compensation Considerations on Basic Design," *IEEE Transactions on Power Application System*, Vol. PAS-90, No. 5, September 1971, pp. 2009-2019.

[11] J. H. Seo, C. H. Choi and D. S. Hyun, "A New Simplified Space-Vector PWM Method for Three-Level Inverter," *IEEE Transactions on Power Electronics*, Vol. 16, No. 4, July 2001, pp. 545-550.

[12] E. Teresa and J. A. Pomilio, "Shunt Active Power Filter Synthesizing Resistive Load," *IEEE transactions on Power Electron*, Vol. 17, No. 2, March 2002, pp. 273-278.

